Changes in the Jahn-Teller distortion at the metal-insulator transition in CMR manganites $(Pr, Nd)_{0.7}(Sr, Ca)_{0.3}MnO_3$

1999 J. Phys.: Condens. Matter 11 109

(http://iopscience.iop.org/0953-8984/11/1/009)

J. Phys.: Condens. Matter **11** (1999) 109–120. Printed in the UK PII: S0953-8984(99)94480-6

Changes in the Jahn–Teller distortion at the metal–insulator transition in CMR manganites $(Pr, Nd)_{0.7}(Sr, Ca)_{0.3}MnO_3$

O Toulemonde†, F Millange†, F Studer†, B Raveau†, J-H Park‡ and C-T Chen§

† Laboratoire CRISMAT, CNRS-UMR 6508, ISMRA, boulevard du Maréchal Juin, 14050 Caen Cédex, France

‡ NSLS Brookhaven National Laboratory, Upton, NY 11973-5000, USA

§ SRRC, 1 R & D Road VI, Hsinchu 30077, Taiwan, People's Republic of China

Received 22 May 1998, in final form 10 September 1998

Abstract. CMR manganites $(Pr, Nd)_{0.7}(Sr, Ca)_{0.3}MnO_3$ were studied by x-ray absorption spectroscopy at the O K-edge above and below the transition temperature T_C. In compounds which keep the insulating behaviour in the whole temperature range, the prepeak at the O K-edge remains unique upon cooling even in the case of the presence of a paramagnetic–ferromagnetic transition. In compounds showing a spontaneous transition from a paramagnetic–insulating state to a ferromagnetic–metallic one, the prepeak at the O K-edge is split into two components. A crystal field analysis of this behaviour is proposed based on the assumption of a strong reduction, upon cooling, of the octahedral distortion due to the dynamic Jahn–Teller splitting present above T_C. This reduction of the crystal field distortion at T_C is correlated to the transition to the metallic state and to the presence of the magneto-resistant effect.

1. Introduction

Extensive studies of the manganese oxide perovskites $Ln_{1-x}AxMnO_3$ (Ln = Re; A = Ca, Sr or Ba) have been carried out especially in the past two years after the discovery of giant or even colossal magneto-resistance (CMR) in these compounds [1–8].

Such colossal negative magneto-resistance properties originate from a double exchange (DE) mechanism between Mn(III) and Mn(IV) species [9–11] which has been proposed to create the ferromagnetism in competition with the superexchange mechanism inducing antiferromagnetic ordering. Like the HTC superconductors, the manganese oxides are highly correlated systems in which the metallic properties are created by hole doping: as a consequence a metallic conductivity can be induced at low temperature which could be due to doping holes in a 2p oxygen band. The antiferromagnetic coupling of these holes to the Mn^{3+} would be at the origin of the ferromagnetic ordering that appears in these oxides. In support of the double exchange model, J-H Park *et al* have observed recently a spin dependence of the Fermi level by high resolution spin resolved photoemission on $La_{0.7}Sr_{0.3}MnO_3$ thin films [12]. These results are in agreement with spin polarized band structure calculations [13] which suggest strongly a semi-metallic behaviour for the lanthanum manganites below T_C.

Besides the DE mechanism, based on the possible existence of dynamic Jahn–Teller distortion of the MnO_6 octahedra, a polaronic type model has recently been proposed by Millis and coworkers [14]. Neutron diffraction studies of these manganites showing structural

0953-8984/99/010109+12$19.50

evolution [15, 16], and XAS studies at the Mn L_3-edge [17, 18] showing changes in the local distortion of the MnO_6 octahedra support strongly this model. But, to date, the variations of the octahedron distortion $D = (d_{Mn-O\ apical}/d_{Mn-O\ equatorial})$ at T_C as recorded by neutron diffraction remain weak, in the range 1.01 to 1.005, and are not sufficient to induce strong atomic level shifts which could account for the huge variations of resistivity observed at the transition in some manganites like the praseodymium ones [4–19]. In fact neutron diffraction data provide only information about the static Jahn–Teller distortion in those oxides.

A strong electron–phonon interaction arising from the Jahn–Teller splitting of the outer Mn d level would play a crucial role. In order to check the existence of such a dynamic Jahn–Teller effect, we have performed an x-ray absorption spectroscopy study at the oxygen K-edge of some CMR manganites. This technique is indeed able to give a reliable picture of the first empty valence states above the Fermi level, due to its characteristic interaction time ($\approx 10^{-15}$ s) which is smaller than the typical phonon period in solids ($\approx 10^{-13}$ s). In this work we show using XAS that a significant decrease of the Jahn–Teller distortion of the manganese octahedra appears at the FMM–PMI transition in CMR manganites $(Pr, Nd)_{0.7}(Sr, Ca)_{0.3}MnO_3$.

2. Experiment

The rare earth manganites $Ln_{0.7}A_{0.3}MnO_3$ (Ln = Pr, Nd) were prepared in the form of sintered pellets following a classical method of solid state chemistry. Thorough mixtures of oxides CaO, $SrCO_3$, Mn_2O_3, Nd_2O_3 or Pr_6O_{11} were first heated in air at 950 °C for 12 hours. The samples were then pressed into pellets and sintered first at 1200 °C and then at 1500 °C for 12 hours in air. X-ray powder diffraction measurement showed single phase patterns.

Magnetization curves $M(T)$ were established with a vibrating sample magnetometer. Samples were first zero field cooled and then the magnetic field was applied at 5 K. Measurements were carried out under warming. Resistance measurements were performed with the four probe technique on sintered bars with $2 \times 2 \times 10$ mm^3 dimensions. Magneto-resistance measurements were performed with a Quantum Design physical property measurement system (PPMS). Resistance was measured with decreasing temperature in zero magnetic fields.

The x-ray absorption study of these phases was performed systematically on the samples previously studied for their transport and magnetic properties [19, 20]. X-ray absorption spectra at O K-edges and Mn $L_{2/3}$-edges were recorded using linear polarized light at the Dragon beamline (U4B) of the NSLS (BNL, USA) respectively in the fluorescence detection mode and total electron yield. The base pressure in the spectrometer chamber was better than 10^{-9} mbar when the sample was cleaved and was maintained below this value during the measurement time. The energy resolution using a slit width of 10 μm was estimated to 0.11 eV at O K-edges.

A standard procedure has been adopted to remove the background contribution from the pre-edge baseline of the spectra. Then the normalization for the various studied compounds was obtained by equalizing the integrated area under the high energy part of the spectra also called covalent spectra between 532 and 550 eV.

3. Results

Two perovskites, $PrMnO_3$ and $CaMnO_3$, were taken as a reference for this XAS study allowing Mn(III) and Mn(IV) to be characterized respectively. The determination of the Mn(III)/Mn(IV)

ratio by chemical titration leads to $PrMnO_{3.10\pm0.05}$, showing that the majority of manganese is trivalent but with some amount of tetravalent manganese, and to $CaMnO_{3.00\pm0.05}$ showing that, for this phase, the majority of manganese is tetravalent.

Stoichiometric $PrMnO_3$ exhibits an orthorhombic distorted structure (SG: *Pnma*) and a transition to an antiferromagnetic order at $T_N = 91$ K [21]. The electron transport and magnetic properties of the overstoichiometric $PrMnO_{3.10\pm0.05}$ are shown in figure 1(a) and (b) showing that the compound remains insulating in the whole temperature range but exhibits a weak transition to a ferromagnetic state at 85 K in agreement with the presence of 20% amount of Mn^{4+} (figure 1). $CaMnO_3$ has been shown to be an antiferromagnetic insulator in its orthorhombic form (*Pnma*) at RT in agreement with recent magnetic full LSDA calculations [13].

The thermal variations of resistance under no magnetic field are shown in figure 2(a) for $Pr_{0.7}Sr_{0.3}MnO_3$ ($T_C = 250$ K) and $Pr_{0.7}Ca_{0.15}Sr_{0.15}MnO_3$ ($T_C = 175$ K) and in figure 2(b) for $Nd_{0.7}Ca_{0.3}MnO_3$ ($T_C = 120$ K). All these compounds present a paramagnetic state to ferromagnetic state transition with cooling temperature.

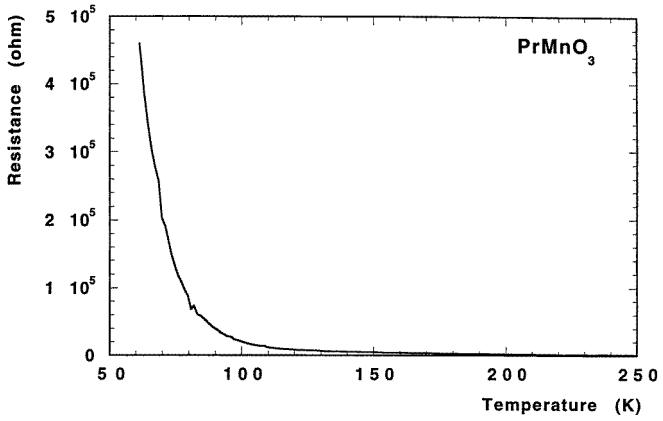

(a)

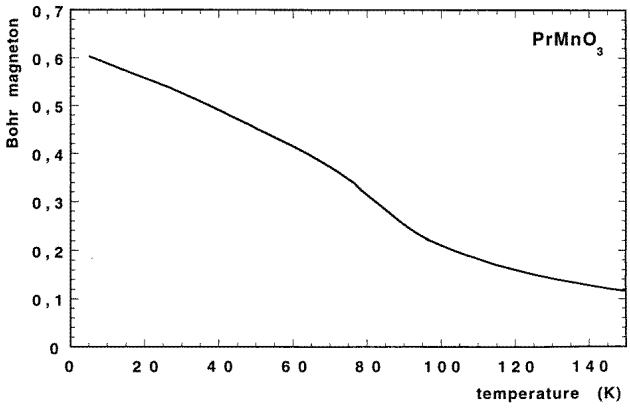

(b)

Figure 1. (a) Thermal variation of resistance for overstoichiometric $PrMnO_{3.1}$; (b) thermal variation of magnetization showing a ferromagnetic behaviour for $T_C = 85$ K.

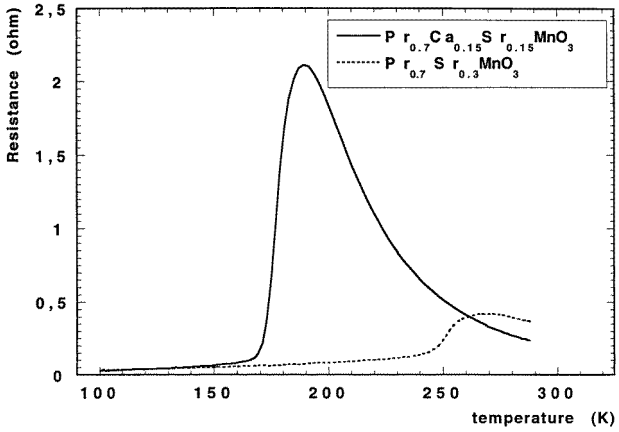

(a)

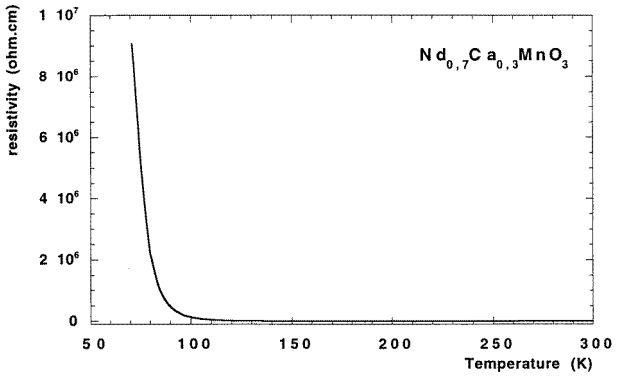

(b)

Figure 2. Thermal variations of resistance showing the magneto-resistance at T_C for (a) $Pr_{0.7}Sr_{0.3}MnO_3$ ($T_C = 250$ K) and $Pr_{0.7}Ca_{0.15}Sr_{0.15}MnO_3$ ($T_C = 175$ K) and (b) $Nd_{0.7}Ca_{0.3}MnO_3$ ($T_C = 120$ K).

The O K-edges of two reference oxides, $PrMnO_3$ and $CaMnO_3$, and of a CMR manganite, $Pr_{0.7}Ca_{0.15}Sr_{0.15}MnO_3$, recorded at room temperature are compared in figure 3. As shown previously by de Groot and coworkers [22] the pre-edge structure (<532 eV) at the O K-edge for transition metal oxides is linked to the metal 3d through hybridization with the O 2p orbitals (figure 4(a)).

As expected, the $Pr_{0.7}Ca_{0.15}Sr_{0.15}MnO_3$ edge at RT exhibits a single round shape prepeak corresponding to an electronic configuration in between the limits Mn^{3+} and Mn^{4+}. The holes induced by doping in the Mn 3d orbitals give the increase of intensity of the low energy peak in an electronic configuration similar to the one of $CaMnO_3$. As can be observed in figure 3, the relative intensity of the prepeak is linked to the hole density in the Mn(3d)–O(2p) molecular orbitals in agreement with the photoelectric absorption rules.

The oxygen K-edge of $PrMnO_3$ was recorded at two temperatures, 10 and 300 K (figure 5). No significant change either in the prepeak or in the valence band structures can be observed at low temperature with respect to RT except for a small narrowing of the peak width as expected from a decrease of the Debye–Weller factor. Especially the double peak structure of the prepeak

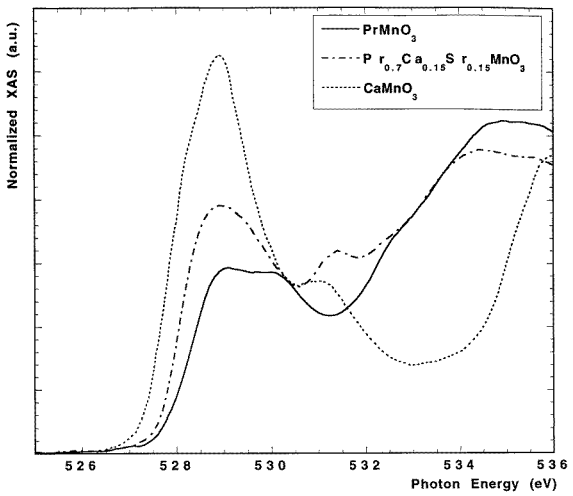

Figure 3. Oxygen K-edges recorded in fluorescence yield mode at room temperature of two reference manganites, $PrMnO_{3.1}$ and $CaMnO_3$, and of a colossal magneto-resistant compound $Pr_{0.7}Ca_{0.15}Sr_{0.15}MnO_3$ ($T_C = 175$ K). The prepeak intensity is correlated to the doping hole densities in the Mn d shell. The prepeak at 529 eV indicates the t_{2g}^3 configuration of Mn(IV) ($3d^3$) which is present also in the spectrum of $PrMnO_{3.1}$ in agreement with the oxygen overstoichiometry.

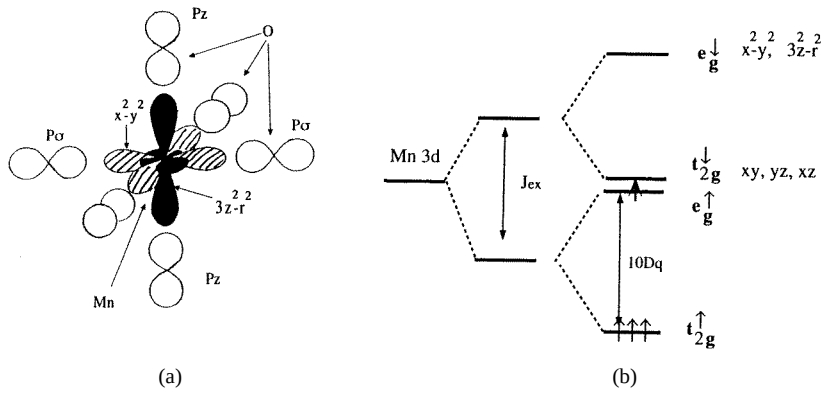

Figure 4. (a) Perspective view of the octahedral environment of Mn with the Mn(3d) and O(2p) atomic orbitals involved in the σ bonding; (b) a schematic drawing of molecular orbitals based on Mn d orbitals in a distorted octahedral crystal field in Mn^{3+} rich compounds.

is preserved at the probed temperatures despite the existence of a ferromagnetic ordering at $T_C = 85$ K. $PrMnO_3$ behaves like small-gap insulators in the whole temperature range in agreement with its filled valence band structure. The absence of any significant change in the electronic structure within the energy resolution of the U4B experiment ($\Delta E = \pm 0.1$ eV) suggests that no significant change of the Jahn–Teller effect occurs at T_C.

Conversely the O K-edges of $Pr_{0.7}Sr_{0.3}MnO_3$ ($T_C = 250$ K) and $Pr_{0.7}Ca_{0.15}Sr_{0.15}MnO_3$ ($T_C = 175$ K) sinters show a totally different behaviour upon cooling from room temperature (figure 6(a) and (b)). For both compounds, below T_C, a double peak structure is clearly observed at 528.8 eV and 529.6 eV, correlated to an edge shift of 0.2 eV towards low energy. Although the edge change around T_C needs to be more precisely analysed, the correlation

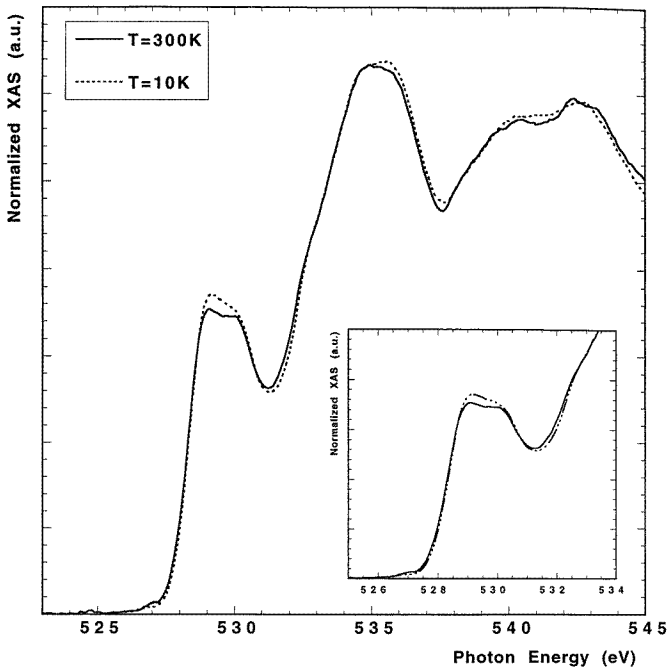

Figure 5. Oxygen K-edges recorded in fluorescence yield mode at room temperature and 10 K of $PrMnO_{3.1}$ showing no significant changes of either the prepeak (below 532 eV) or the valence spectrum (above 532 eV).

between the PMI–FMM transition and the occurrence of a double peak structure seems to be established. Moreover such a double peak shape of the prepeak at the O K-edge was also observed by Pellegrin *et al* [23] in $La_{1-x}Sr_xMnO_3$ compounds for $x > 0.18$ at low temperature in the ferromagnetic/metal-like state. But these authors did not check for a prepeak change with temperature.

Another sample with nominal composition $Nd_{0.7}Ca_{0.3}MnO_3$ was recorded in the same experimental conditions. This compound shows a particular behaviour since it keeps insulating in a large temperature range (5–240 K) due to charge ordering of Mn^{3+} and Mn^{4+} cations but exhibits a ferromagnetic ordering at $T_C = 120$ K as shown by magnetization measurements and neutron diffraction experiments [20, 24]. Indeed, as for the reference oxide $PrMnO_3$, the prepeak at the O K-edge of $Nd_{0.7}Ca_{0.3}MnO_3$ shows no significant change for the three temperatures used throughout this work (10, 100 and 300 K: figure 7). This result is in agreement with the absence of any significant change of the Mn–O distances at T_C as seen by neutron diffraction. It also shows that the ferromagnetic ordering of manganese cations does not induce systematically a transition to a metallic state, in contrast to what is observed in many other manganites following the double exchange model. Furthermore it shows that a correlation holds between the occurrence of a metallic state and the observation of a double peak structure at the O K-edge.

4. Models

The valence band structure of manganese perovskites has been investigated by many authors using band structure calculations (ASW, TB–LMTO) either in the LSDA (local spin density

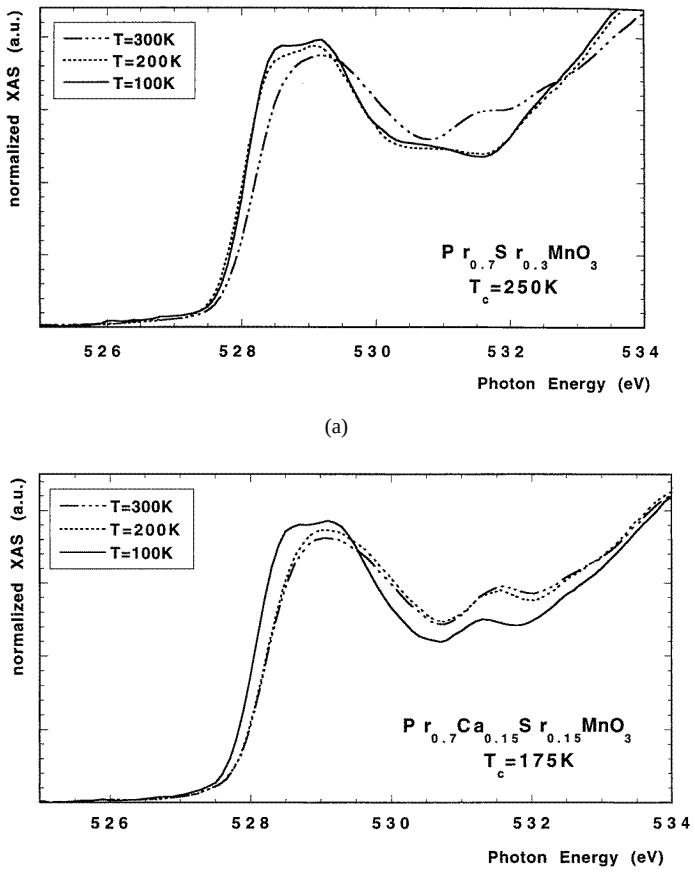

Figure 6. Oxygen K-edges recorded in fluorescence yield mode at room temperature, 200 K and 100 K of two CMR manganites, $Pr_{0.7}Sr_{0.3}MnO_3$ and $Pr_{0.7}Ca_{0.15}Sr_{0.15}MnO_3$, showing the significant change of the prepeak below T_C i.e. in the ferromagnetic–metallic domain.

approximation) or LSDA + U formalisms [13, 25–28]. The splitting of spin-up and spin-down electronic levels are obtained either through intrashell Coulomb repulsion (Hubbard's parameter) for the LSDA + U or through an exchange interaction calculated in the Stoner model of ferromagnetic metals for ASW calculations. Both methods correspond to different approximations but give similar descriptions of the electronic DOS structure which fit properly the so-called valence part of the spectra ($E_{ph} > 532$ eV). The main result of these single electron calculations is to show that manganese perovskites behave like semi-metals with a metallic spin-up and an insulating spin-down band structure. This semi-metallic band structure was confirmed recently by spin resolved photoemission spectroscopy [12].

But there exist also 'cluster' calculations of the complete set of molecular orbitals limited to a few atoms around the transition metal which allow a better understanding of the crystal field effect and which better describe the prepeak behaviour at the O K-edge ($E_{ph} < 532$ eV). First X_α cluster calculations were published earlier by Kurata and Colliex [29] for the analysis of electron energy loss (EELS) at O K-edges of manganese oxides. They already showed that a shift in the Mn orbital configurations occurs between Mn^{3+} and Mn^{4+} due to the relative

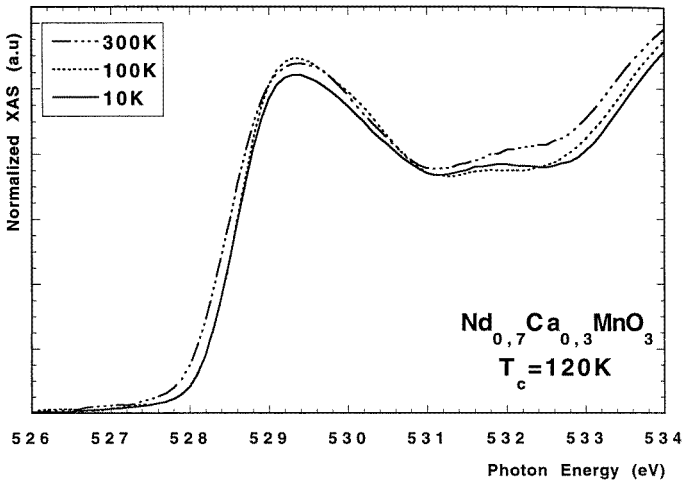

Figure 7. Oxygen K-edges recorded in fluorescence yield mode at room temperature, 100 K and 10 K of the manganite $Nd_{0.7}Ca_{0.3}MnO_3$ exhibiting charge ordering below 240 K, a ferromagnetic transition at 120 K and an insulating behaviour in the whole temperature range.

interplay of the exchange interaction parameter J_{exc} and of the crystal field $10Dq$. The $10Dq$ and J_{exc} values were estimated from this work to be 2.4 and 3.4 eV for Mn^{3+} and 3.3 and 3.0 eV for Mn^{4+}. An example of such a cluster calculation is presented for MnO_6 octahedra in cubic symmetry O_h in figure 4(a). This picture does not take into account the splitting of e_g molecular orbitals due to distortion of the manganese octahedra. The orbital splitting depends mainly on the difference $J_{exc} - 10Dq$, which decreases with increasing Mn^{4+} amount and crystal field symmetry (figure 8). For strong distortions, the splitting of e_g and t_{2g} orbitals (figure 8(C) and 8(D)) leads to energy differences between electronic states smaller than the monochromator resolution and will thus result in a broadening of the prepeak line.

In the case of the octahedral Mn^{3+} cation ($3d^4$ electronic configuration), J_{exc} is larger than $10Dq$ [29] and the spin-up levels at low energy are separated from the spin-down levels such that the fourth electron occupies the $e_g^{\uparrow}$ orbital in a classical schema already proposed for manganites (figure 4(b)). Thus the high energy peak at 530 eV (figure 3) on the O K-edge of $PrMnO_3$ corresponds to the empty spin-up $e_g^{\uparrow}$ orbitals mixed and not separated from the $t_{2g}^{\downarrow}$ ones whereas $e_g^{\downarrow}$ orbitals are rejected at higher energies in the valence band spectrum (figure 3). The presence of the first peak at 529 eV, at the same energy as the one of $CaMnO_3$, was addressed previously by Park *et al* [30]: it was attributed to the $t_{2g}^{\downarrow}$, $e_g^{\uparrow}$ orbitals of Mn^{4+} whose presence originates from the oxygen overstoichiometry δ in the formula $PrMnO_{3.1}$. Figure 8(D) holds for Mn^{3+} in a Jahn–Teller distorted crystal field, for instance $LaMnO_3$ or $PrMnO_3$, in which J_{exc} is larger than $10Dq$.

For Mn^{4+} in octahedral coordination ($3d^3$ electronic configuration), the exchange interaction J_{exc} is smaller than $10Dq$ and the three electrons of the Mn^{4+} cation ($3d^3$ electronic configuration) fill the lowest lying $t_{2g}^{\uparrow}$ molecular orbitals. Empty $t_{2g}^{\downarrow}$, $e_g^{\uparrow}$ orbitals are not resolved due to the close values of the crystal field splitting $10Dq$ and of the exchange energy J_{exc}. Thus the intense and wide prepeak at 529 eV should correspond to the $1s \rightarrow 3d(t_{2g}^{\downarrow} e_g^{\uparrow})$ electronic transitions whereas the second small peak at 531.5 eV should correspond to the $1s \rightarrow 3d(e_g^{\downarrow})$ one. Figure 8(A) holds for Mn^{4+} in a slightly distorted crystal field, for instance $CaMnO_3$, in which J_{exc} is smaller than $10Dq$.

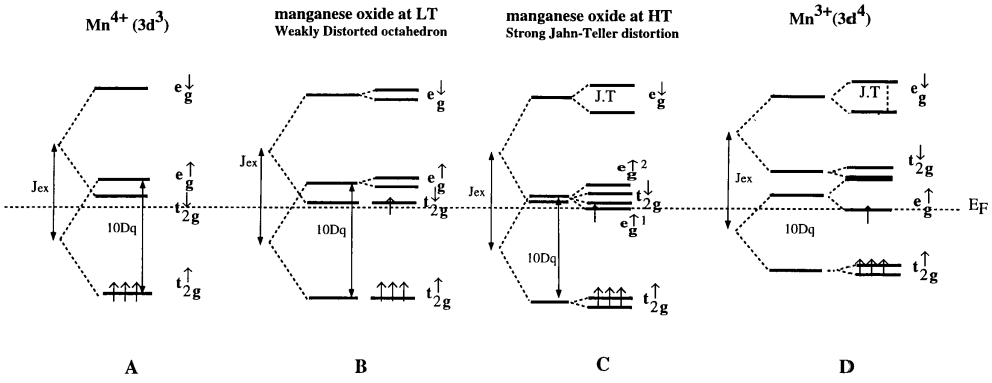

Figure 8. Schematic energy level diagram of molecular orbitals for Mn(III) (D), Mn(IV) (A) and the mixed valent CMR compounds (B and C) studied in this work. The respective values of the exchange interaction parameter J_{exc} and of the crystal field strength $10Dq$ were estimated previously by Kurata *et al* [29] from X_α cluster calculations.

The O K-edges of $Pr_{0.7}Sr_{0.3}MnO_3$, $Pr_{0.7}Ca_{0.15}Sr_{0.15}MnO_3$ and $Nd_{0.7}Ca_{0.3}MnO_3$ at RT present a first intense peak at 529 eV which can be attributed to holes in a non-resolved set of $e_g^{\uparrow}$ and $t_{2g}^{\downarrow}$ molecular orbitals in agreement with the level diagram of figure 8(C) which holds for a strong Jahn–Teller distortion around manganese. In a strong axial distortion of the octahedra, the splitting of e_g orbitals can be as high as 1 eV due to their large σ hybridization with oxygen 2p orbitals. A splitting of t_{2g} orbitals is also created by the crystal field distortion but weaker than the one of e_g orbitals due to the weaker π hybridization. Also for the same reasons, the e_g orbitals will form wide bands whereas t_{2g} orbitals will be limited to narrower levels. The $e_g^{\downarrow}$ orbital thus appears at 531.5 eV with an intensity higher for $CaMnO_3$ than for the substituted compounds. This may be due to a larger distortion of MnO_6 octahedra in the latter compounds than in $CaMnO_3$ resulting in a dispersion of $e_g^{\downarrow}$ density of states as shown by band structure calculations.

But, below T_C in the substituted manganites, one must introduce a reduction of the Jahn–Teller distortion around Mn^{3+} cations taking into account the results of neutron diffraction [15, 16]. These results indicate a small reduction of the MnO_6 distortion occurs at T_C. For XAS, the reduction of the dynamic Jahn–Teller effect, upon cooling below T_C, will reduce considerably the splitting of e_g and t_{2g} molecular orbitals inducing the configuration pictured in figure 8(B) with $J_{exc} > 10Dq$. This would result in a clear separation of the $t_{2g}^{\downarrow}$ levels, which appear at 529.5 eV, from the $e_g^{\uparrow}$ levels at 530.3 eV.

5. Discussion

Within this general framework, one can now understand that, upon cooling below T_C, the reduction of the strong dynamic Jahn–Teller distortion, existing at higher temperatures, can cancel the splitting of $e_g^{\uparrow}$ and $t_{2g}^{\downarrow}$ (σ and π overlapping respectively) levels allowing them to be well separated in the pre-edge feature. Taking into account that the exchange interaction parameter J_{exc} is smaller than the crystal field strength $10Dq$ as in Mn^{4+} rich compounds, one has to assert that the lowest unoccupied molecular orbital (LUMO) is a spin-down $t_{2g}^{\downarrow}$ partly filled with electron (hole) depending on the substitution amount.

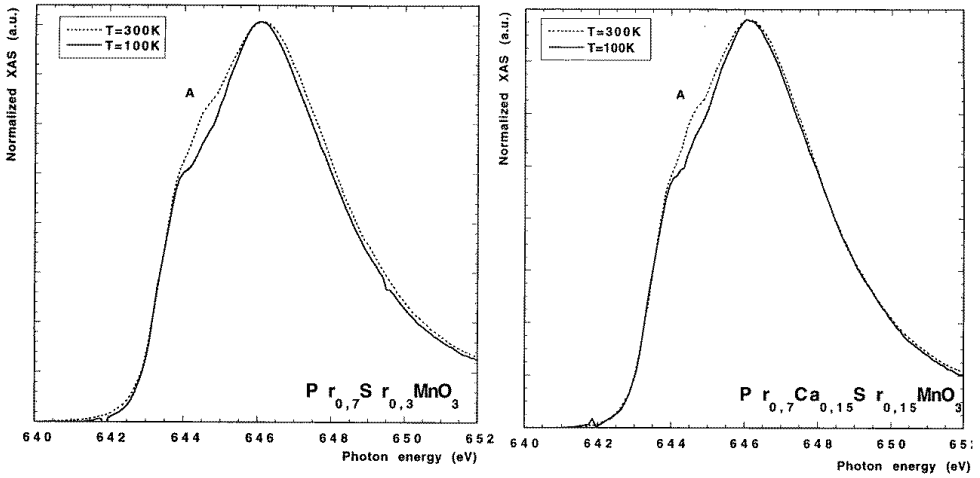

(a) (b)

Figure 9. Manganese $L_{2/3}$-edges recorded in total electron yield mode at room temperature and 100 K of two CMR manganites, $Pr_{0.7}Sr_{0.3}MnO_3$ and $Pr_{0.7}Ca_{0.15}Sr_{0.15}MnO_3$, showing the significant change below T_C i.e. in the ferromagnetic–metallic domain.

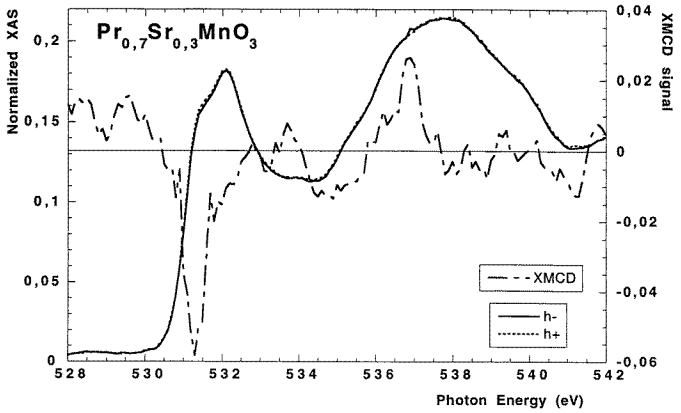

Figure 10. XMCD effect at O K-edge on a $Pr_{0.7}Sr_{0.3}MnO_3$ sinter as observed using the DRAGON beamline of ESRF equipped with the Flipper Magnet system. The dichroic signal is observed for the first low-energy prepeak assigned to O 2p hybridized Mn 3d states with t_{2g} spin-down character.

This conclusion is supported by former XAS observations at Mn L_3-edges [17, 18] which have shown the presence of changes upon cooling through T_C in agreement also with the existence of a Jahn–Teller distortion. However no splitting of Mn 3d–O 2p bands with temperature was observed in the valence band photoemission of the $La_{0.66}Ca_{0.33}MnO_3$ compound [30]. The observation of changes in the Mn 3d photo-absorption spectra with temperature is also an important issue since the Jahn–Teller distortions must move the manganese 3d as well as the oxygen 2p levels. In order to ascertain the correlation between the transition to a metallic behaviour and the reduction of the Jahn–Teller distortions at T_C, we have also recorded the Mn L_3-edges of $Pr_{0.7}Sr_{0.3}MnO_3$ and $Pr_{0.7}Ca_{0.15}Sr_{0.15}MnO_3$ for two temperatures, 100 and 300 K, as shown in figures 9(a) and (b) respectively. The decrease of the

line marked A is clearly observed on both edges below T_C. Using the TT-multiplet calculations of low- and high-spin Mn^{3+} made by de Groot [31], the A peak reduction in the Mn L_3-edge was attributed to an increase of the low-spin configuration below T_C [17, 18].

Also recent XMCD experiments at the O K-edge performed on $Pr_{0.7}Sr_{0.3}MnO_3$ sinter on the DRAGON beamline of ESRF (Grenoble, France) have shown that, below T_C, the electronic transitions corresponding to the first prepeak are majority spin down in agreement with a predominant $t_{2g}^{\downarrow}$ character (figure 10). Finally our results are consistent with ASW band structure calculations for $CaMnO_3$ which showed that the $t_{2g}^{\downarrow}$ level is the LUMO in which is located the Fermi level upon electron doping.

At the level of the electron transport behaviour, this picture is also consistent at low temperature with a metallic conduction in narrow π molecular orbitals proposed by many authors. Thus, above transition temperatures, the insulating behaviour could only be created by a reduction of the band width induced by the strong distortion of the MnO_6 octahedra. The increase of the Mn–O distances as well as the deviation of the O–Mn–O angle from 180° can reduce considerably the Mn(3d)–O(2p) overlap and lead to carrier localization.

6. Conclusion

High resolution soft x-ray absorption spectroscopy at the O K-edge of manganese oxides, $PrMnO_3$ and $CaMnO_3$ and CMR praseodymium and neodymium manganites, was performed at the NSLS (BNL, Brookhaven) for temperatures ranging from 10 to 300 K. Analysis of the pre-edge feature (below 532 eV) was realized assuming that this pre-edge corresponds to electronic transitions to holes in σ and π molecular orbitals, due to hybridization of Mn 3d and O 2p orbitals, split by the crystal field and exchange interaction. In manganites exhibiting the PI–FM transition and colossal magneto-resistance, the preedge splits into two components below T_C whereas the O K-edges of $PrMnO_3$, $CaMnO_3$ and $Nd_{0.7}Ca_{0.3}MnO_3$ do not show any change in the pre-edge shape between 10 K and room temperature. However the latter compound exhibits a ferromagnetic ordering below $T_C = 120$ K keeping an insulating behaviour due to charge ordering. Thus the transition from an insulating to a metallic state as T decreases seems to be correlated to the existence of a splitting of the oxygen pre-edge corresponding to a decrease of the crystal field distortion around the manganese. This demonstrates that a significant increase of the crystal field distortion around the manganese transition should take place at the FMM–PMI in agreement with the previous neutron diffraction results [15, 16]. This effect is much more amplified here due to the XAS technique whose interaction time is smaller than the phonon period. In other words, these results support strongly the existence of a dynamic Jahn–Teller distortion of the MnO_6 octahedron expected from the polaronic model of Millis and coworkers [14]. It is worth noting that they are not contradictory with the double-exchange model of de Gennes [11] but give a complementary description allowing us to account for huge variations of resistance at the FMM–PMI transition.

References

[1] Kuster R M, Singleton J, Keon D A, Greedy R M and Hayes W 1989 *Physica* B **155** 362
[2] Von Hemmolt R, Wecker J, Holzapfel B, Schultz L and Samwer K 1993 *Phys. Rev. Lett.* **71** 2331
[3] Ju H L, Kwon C, Li Q, Greene R L and Venkaten T 1994 *Appl. Phys. Lett.* **65** 2108
[4] Maignan A, Simon Ch, Caignaert V and Raveau B 1995 *Solid State Commun.* **96** 623
[5] Mahesh R, Mahendiran R, Raychaudhury A K and Rao C N R 1995 *J. Solid State Chem.* **114** 297
[6] Jin S, O'Bryan H M, Tiefel T H, McCormack M and Rhodes W W 1995 *Appl. Phys. Lett.* **66** 382
[7] Maignan A, Martin C and Raveau B 1997 *Z. Phys.* B **102** 19
[8] Martin C, Maignan A and Raveau B 1996 *J. Mater Chem.* **6** 1245

[9] Zener C 1951 *Phys. Rev.* **82** 403
[10] Anderson P W and Hasegawa H 1955 *Phys. Rev.* **100** 975
[11] De Gennes P G 1960 *Phys. Rev.* **118** 141
[12] Park J H, Vescovo E, Kim H J, Kwon C, Ramesh R and Venkatesan T 1998 *Nature* **392** 794
[13] Picket W E and Singh D J 1996 *Phys. Rev.* B **53** 1146
[14] Millis A J, Litlewood P B and Shraiman B I 1995 *Phys. Rev. Lett.* **74** 5144
Millis A J, Shraiman B I and Mueller R 1996 *Phys. Rev. Lett.* **77** 175
[15] Caignaert V, Suard E, Maignan A, Simon Ch and Raveau B 1996 *J. Magn. Magn. Mater.* **153** L260
[16] Garcia-Munoz J L, Suaaidi M, Fontcuberta J and Rodriguez-Carvajal J 1997 *Phys. Rev.* B **55** 34
[17] Studer F, Toulemonde O, Caignaert V, Srivastava P, Goedkoop J and Brookes N 1997 *Proc. 9th Int. Conf. on X-Ray Absorption Fine Structure, J. Physique Coll.* IV **7** C2 529
[18] Toulemonde O, Studer F, Lobet A, Ranno L, Maignan A, Pollert E, Nevriva M, Pellegrin E, Brooks N B and Goedkoop J 1998 *J. Magn. Magn. Mater.* at press
[19] Raveau B, Maignan A and Caignaert V 1995 *J. Solid State Chem.* **117** 424
[20] Millange F, Maignan A, Caignaert V, Simon Ch and Raveau B 1996 *Z. Phys.* B **101** 169
[21] Quezel-Ambrunaz S 1968 *Bull. Soc. Fr. Minéral. Cristallogr.* **91** 339
[22] de Groot F M F, Grioni M, Fuggle J C, Ghijsen J, Sawatzky G A and Petersen H 1989 *Phys. Rev.* B **40** 5715
[23] Pellegrin E, Tjeng L H, de Groot F M F, Hesper R, Flipse C F J, O'Mahony J D, Moritomo Y, Tokura Y, Chen C T and Sawatzky G A 1997 *Proc. 9th Int. Conf. on X-Ray Absorption Fine Structure, J. Physique Coll.* IV **7** C2 405
[24] Caignaert V, Millange F, Hervieu M, Mather G, Raveau B, Suard E, Laffez P and Van Tendeloo G *Phys. Rev.* B at press
[25] Satpathy S, Popovic Z S and Vukajlovic F R 1996 *Phys. Rev. Lett.* **76** 960
[26] Anisimov V I, Elfimov I S, Korotin M A and Terakura K 1997 *Phys. Rev.* B **55** 15 494
[27] Sawada H, Morikawa Y, Terakura K and Hamada N 1997 *Phys. Rev.* B **56** 12 154
[28] Matar S, Studer F, Siberchicot B, Subramaniam M A, Demazeau G and Etourneau J *Eur. Phys. J. Appl. Phys.* accepted for publication
[29] Kurata H and Colliex C 1993 *Phys. Rev.* B **48** 2101
[30] Park J H, Chen C T, Cheong S-W, Bao W, Meigs G, Chakarian V and Idzerda Y U 1996 *Phys. Rev. Lett.* **76** 4215
[31] de Groot F M F 1991 *Thesis* University of Groningen